Springer

KSME

Journal of Mechanical Science and Technology 25 (7) (2011) 1675~1685
www.springerlink.com/content/1738-494x
DOI 10.1007/s12206-011-0503-z

Impact noise radiated by collision of two spheres: Comparison between numerical simulations, experiments and analytical results †

K. Mehraby[1], H. Khademhosseini Beheshti[2,*] and M. Poursina[2]

[1]*Adjunct faculty, Islamic Azad University of Majlesi, Majlesi, 863165-6451, Iran*
[2]*Faculty of Engineering, Department of Mechanical Engineering, University of Isfahan, HezarJarib Ave., Isfahan, 81746-73441, Iran*

(Manuscript Received October 5, 2010; Revised March 1, 2011; Accepted March 8, 2011)

Abstract

Impact is very common source of noise in the industries. The impacts can be visible, such as forging, and can be invisible, such as impacts due to clearance of hinges. As a result of this generality, the control of impact noise needs more attention. Reduction of this tiresome noise needs enough perception about the impact. A study of this noise sources presents difficult problems both theoretically and experimentally. This is partly due to the many complex interconnected mechanical phenomena that occur and partly due to the fact that usual steady-state techniques of analysis cannot be applied. In such complex problems numerical techniques can help to acousticians. To gain some insight into this source of sound, in this paper collision of two steel spheres are studied with finite element method (FEM). Then the FEM results were compared with experiments to show authority of this numerical method to simulate impact noises. FEM results show that if the vibrational modes are excited by impact, the vibrational modes can be as effective as rigid body motion.

Keywords: Impact noise; Vibration; Collision; FEM

1. Introduction

When two bodies collide, their kinetic energy transforms to another forms of energy such as heat, plastic deformation, fracture and sound. These energy transforms take place in a very short duration, so that it always makes the impact study very cumbersome.

The mechanical impact phenomena can happen in riveting, forging, printing and gear teeth. Although the contribution of acoustic energy is negligible in mentioned energy transforms, the sensitivity of humane auditory system forces designers to attend the noise radiated from their designs.

The impact usually exists in various industries. However, collecting the experimental study of the phenomena is not easy because of high speed of propagation of elastic waves in solid structure. Several papers on the behavior of propagating transient flexural waves in impacted plates have been reported [1-3]. Some manuscripts are surveyed sound radiated from impacted plates [4-6]. Olofsson et al. [7, 8] studied transient bending waves in tubes. Love [9] and Goldsmith [10] also investigated the elastic collision of spheres. Nishimura and Takahashi [11] measured acoustic noise radiated by colliding of two spheres. Koss and Alfredson [12] studied analytically the noise of colliding spheres. Yufang and Zhongfang [13] studied the impact of cylinders and then Richard et al. [14] studied more complex bodies such as cones.

This paper simulates sound radiated form collision of two steel spheres with the finite element method (FEM) then results are compared with analytical methods and experiments. In the first step of numerical method, collision of spheres is simulated and spheres reactions are studied. In the second step, the state variables which were produced in previous step are used to excite the air elements. Exciting is applied based on continuity law.

The experimental and analytical results that used in the paper are extracted from Koss and Alfredson resources [12]. To give theoretical solution Koss and Alfredson analytically calculated acceleration of each sphere utilizing Hertzian's theorem. The velocity potential that is generated by an oscillating sphere in a fluid was given by Rayleigh [15]. They obtained a pressure field by using the velocity potential and then replacing acceleration to it. The general solution is given by superposition of the pressures radiated by each sphere. Following section explains the problem that they studied.

2. Koss and Alfredson's problem

They studied collision between two spheres with 2-inch diameter. The spheres were made by steel with Vicker's hard-

† This paper was recommended for publication in revised form by Editor Yeon June Kang

* Corresponding author. Tel.: +983117934052, Fax.: +983117932746
E-mail address: hamid.beheshti@eng.ui.ac.ir

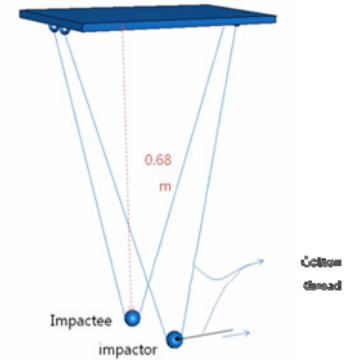

Fig. 1. Schematic of sphere suspension apparatus.

ness of 880. For using in the computer code, they supposed that Young's modulus was 1.95 * 1011 Pascals, the value of Poisson's ratio was 0.28, density of air was 1.184 kg/m3, and Bulk module was 137000 Pascals.

They hung each sphere from a steel channel by two cotton threads shown in Fig. 1. A cotton tread was attached to the rear of impactor sphere. By using the cotton tread the impactor was lifted and then was released. They used an inaudible laser beam velocity measuring device to measure impact velocity and impact duration. They also used a set of microphones to store the created sound pressure around the spheres.

By using Hertzian's theorem and velocity potential, they gave following relation to calculate acoustic pressure in time t and at a place in a direction θ degree from impact axes and r meters from impact point.

$$\begin{aligned} & p(r,\theta,t) \\ & = \frac{\rho_0 f a^3 \cos\theta}{4m(b^4+4l^4)} \frac{1}{2r^2} \left\{ \left(\frac{2r}{a} \right. \right. \\ & \left. - 1 \right) \left[(8l^3 b - 4lb^3) \cos bt' + 8b^2 l^2 \sin bt' \right] \\ & - 4b^4 \sin bt' - (8l^3 b + 4lb^3) \cos bt' \\ & + \left(\frac{2r}{a} - 1 \right) \left[(4b^3 l - 8bl^3) \cos lt' \right. \\ & \left. - (8bl^3 + 4b^3 l) \sin lt' \right] e^{-lt'} \\ & + \left[(4b^3 l - 8bl^3) \cos l\left(t' - \frac{\pi}{2l} \right) \right. \\ & \left. \left. - (8bl^3 + 4b^3 l) \sin l\left(t' - \frac{\pi}{2l} \right) \right] e^{-lt'} \right\} \\ & + \frac{\rho_0 f a^3 \cos\theta}{2mr^2} \sin bt' \end{aligned} \tag{1}$$

where ρ_0 is the density of air, a is the radius of spheres, and m is the mass of spheres. This relation applies only for delay time less than impact duration ($t' \le \tau$). They gave the same relation for the greater times, too [12]. Other above parameters is attained as following:

$$t' = t - \frac{r-a}{c} \tag{2}$$

$$b = \frac{\pi}{\tau} \tag{3}$$

$$l = \frac{c}{a} \tag{4}$$

$$f = k \left[\frac{5mv_0^2}{8k} \right]^{0.6} \tag{5}$$

$$k = \frac{4}{3} \left[\frac{E}{2(1-\nu^2)} \right] \left(\frac{a}{2} \right)^{0.5} \tag{6}$$

where d is the duration of impact, c is the speed of sound in air, v_0 is the impact velocity, E is the Young's modulus, and ν is the Poisson's ratio.

3. Simulation

Almost in all of simulations, when a structure is interacted with air, it is assumed that effect of air on structure is negligible. This simplification is applied because of the difference between the elastic waves speed in air and in the solids. In this simulation the effect of air on sphere is ignored to reduce calculation time. Therefore, the problem is simulated uncoupled. In first step colliding of spheres is simulated and reactions of spheres are studied. In the second step the state variables, which are calculated in the first step, are used to excite the air.

In the simulation, axisymmetry around impact axis as well as symmetry of sphere are assumed.

3.1 Simulation of impact

In acoustic-structure problems, the structural behavior is defined by the virtual work equation.

$$\begin{aligned} & \int_V \delta\boldsymbol{\varepsilon} : \boldsymbol{\sigma}\, dV + \int_V \alpha_c \rho \delta \mathbf{u}^m . \dot{\mathbf{u}}^m\, dV \\ & + \int_V \rho \delta \mathbf{u}^m . \ddot{\mathbf{u}}^m\, dV - \int_{S_t} \delta \mathbf{u}^m . \mathbf{t}\, ds \\ & + \int_{S_{fs}} p \delta \mathbf{u}^m . \mathbf{n}\, ds = 0 \end{aligned} \tag{7}$$

where $\boldsymbol{\sigma}$ is the stress at a point in the structure, p is the pressure acting on the fluid structural interface (Sfs), $\mathbf{n}$ is the outward normal to the structure, ρ is the density of the material, $\mathbf{t}$ is the surface traction applied to the surface of structure (St), $\dot{\mathbf{u}}^m$ is the velocity of a point in the structure, $\ddot{\mathbf{u}}^m$ is the acceleration of a point in the structure, $\delta\mathbf{u}^m$ is a variation displacement field, $\delta\boldsymbol{\varepsilon}$ is the strain variation that is compatible with $\delta\mathbf{u}^m$, and α_c is the mass proportional damping factor that uses Rayleigh damping to define it. For simplicity in this equation, all other loading terms except the fluid pressure and surface traction have been neglected.

It will be seen that acoustic waves are propagated in about one millisecond duration of time. In this paper because of this short duration of time and substance of the spheres, the damping is ignored.

The effects of air on spheres are also ignored. So the only traction that is applied to spheres is applied on contact area and in contact time. To calculate this traction in every increment, the penalty method is used.

In this research the sound created by impact of two spheres

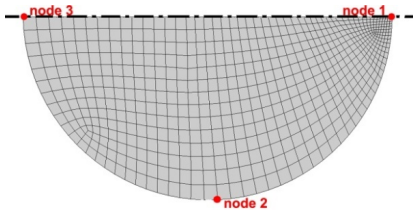

Fig. 2. Finite elements mash of sphere.

is mostly dependent on the surface accelerations. These accelerations are also dependent on the deformations of spheres which are affected by the contact forces. We know that the contact force depends on the relative velocity of spheres rather than the absolute velocity. In this simulation, the relative velocities have been taken into consideration. Therefore, to simulate the problem symmetrically, just one sphere is modeled and this sphere with initial velocity of 0.15 m/s collides with a rigid wall. With this simplification and after discretization of Eq. (7) by using interpolator $\mathbf{u}^m = N^N u^N$, it is possible to rewrite the equation as below:

$$M^{NM}\ddot{u}^M + I^N - P^N = 0. \tag{8}$$

In this equation M^{NM} is the mass matrix, I^N is the internal force vector, and P^N is the external force vector that is calculated as below [16]:

$$\begin{aligned} M^{NM} &= \int_V \rho N^N . N^M dV \\ I^N &= \int_V \beta^N : \boldsymbol{\sigma}\, dV \\ P^N &= \int_S N^N . \mathbf{t}\, dS. \end{aligned} \tag{9}$$

In this equation N^N is the displacement interpolator function, and β^N is the strain interpolator function.

To solve Eq. (7), model is discretized by 650 quadrilateral elements with 4 nodes and one Guassian integration point shown in Fig. 2. Mesh intensity analysis shows that we can reach to appropriate results with less number of elements. Nonetheless to increase care in simulating of contact and better coincidence of solid elements with air elements, in the next step, the mesh with the mentioned number of elements is used. All of the elements in the mesh have less than one millimeter length.

The problem consists of contact constraint; therefore it needs to calculate contact properties in each increment. The integration of Eq. (8) is achieved explicitly to reduce solution costs. The results will be studied in following.

The contact force that was calculated by FEM is compared with Hertzian's theorem to verify simulation. Deresiewicz [17] by using Hertzian's theorem reaches following equations to calculate duration of contact and the maximum contact force in the elastic collision of bodies.

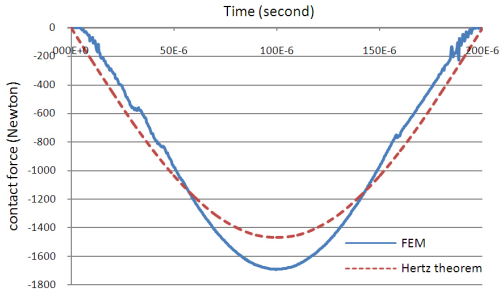

Fig. 3. Contact force.

$$\tau = 2.86\left(\frac{m_*^2}{E_*^2 R_* v_0}\right)^{1/5} \tag{10}$$

$$F = 1.94 E_* R_*^2 \left(\frac{m_* v_0^2/2}{E_* R_*^3}\right)^{3/5}. \tag{11}$$

In these equations v_0 is impact velocity, m_*, E_*, and R_* are effective mass, effective elastic module and effective radius of curvature in contact area, respectively. These parameters are calculated as follows:

$$\begin{aligned} E_* &= \frac{E}{2(1-\nu^2)} \\ R_* &= \frac{r}{2} \\ m_* &= \frac{m}{2}. \end{aligned} \tag{12}$$

Eq. (10) shows that contact period is about 0.2 milliseconds. In addition, Eq. (11) shows that the maximum impact force is 1470 N. By assuming half-sine behavior for contact force [10]. The contact force is shown in Fig. 3. Solid line was taken from FEM results and dash-line was taken from Hertzian's theorem.

This figure shows a good agreement between the simulation and the Hertzian's theorem. Based on the diagram, although both methods give same contact period, the maximum contact force is different.

Based on Euler's equation pressure gradient corresponds to the acceleration [18]. The radial accelerations and acceleration spectrum in node 3, specified in Fig. 2, are plotted on Fig. 4(a) to study the effect of surface deformations of spheres on creation of sound. The acceleration curve is transformed by Fourier series to determine the spectrum. The algorithm of Fourier transform that is used to this expansion is the Fast Fourier Transform (FFT). The natural frequencies of spheres will also be specified in section 4. Compare between Fig. 4(b) and natural frequencies shows that the picks of spectrum curve are merged on natural frequencies.

Because of rapid perturbations on Fig. 4(a), it is not possible to obtain any important result from this figure. The noise with frequencies above 20 kHz does not have any effects on the radiation of audible sounds. Therefore, by using a low-pass integrator filter, noises with frequency above this frequency is

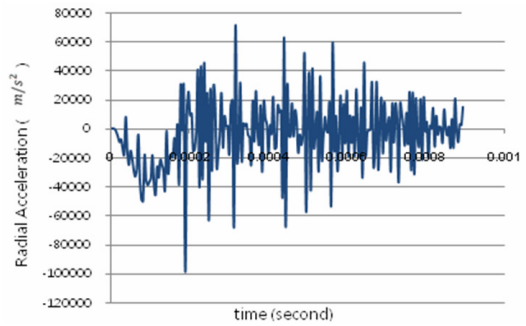

(a)

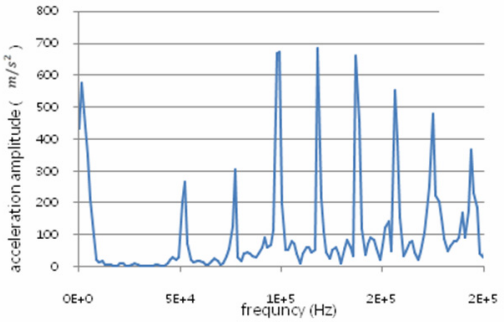

(b)

Fig. 4. (a) Radial acceleration in node 3; (b) acceleration spectra in node 3.

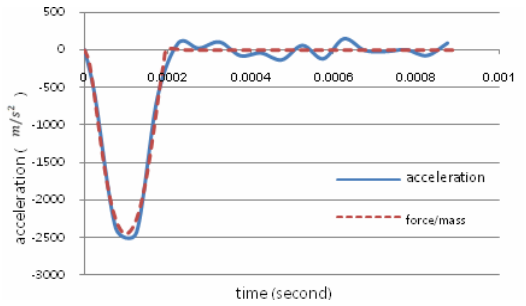

Fig. 5. Filtered radial acceleration of node 3.

omitted from Fig. 4(a). Fig. 5 shows the result of this filtering. In Fig. 5 the solid line shows filtered acceleration and dash-line shows the rigid body acceleration due to the contact force. The rigid body acceleration is calculated by dividing the contact force to the mass of the sphere (535 grams).

Coincidence of the rigid body acceleration and the filtered acceleration shows that the sound is merely radiated due to the rigid body motion. Because only frequency of rigid body motion is in audible range. The acceleration spectrum or vibration modes of spheres show that only the rigid body mode has a frequency in audible range. So, the acceleration spectrum shows that sound radiated due to the rigid body motion, too.

3.2 Acoustic simulation

Acoustical FEM is formulated by studying equilibrium equation for small motions of a fluid. This equation for a compressible, an adiabatic fluid with a velocity-dependent momentum losses is taken to be as Eq. (13) [16].

$$\frac{\partial p}{\partial \mathbf{x}} + \gamma(\mathbf{x},\theta_i)\dot{\mathbf{u}}^f + \rho_f(\mathbf{x},\theta_i)\ddot{\mathbf{u}}^f = 0 \tag{13}$$

where p is the excess pressure in the fluid, $\mathbf{x}$ is the spatial position of the fluid particle, $\dot{\mathbf{u}}^f$ is the fluid particle velocity, $\ddot{\mathbf{u}}^f$ is the fluid particle acceleration, ρ_f is the density of the fluid, γ is the volumetric drag, and θ_i are i independent field variables such as temperature, humidity of air on which ρ_f and γ may depend.

The constitutive behavior of the fluid is assumed to be inviscid, linear, and compressible; so that Eq. (14) can be written.

$$p = -K_f(\mathbf{x},\theta_i)\frac{\partial}{\partial \mathbf{x}}\cdot\mathbf{u}^f \tag{14}$$

where K_f is the bulk modulus of the fluid.

An equivalent weak form for the equation of motion, Eq. (13), is obtained by introducing an arbitrary variational field, δp, and integrating over the fluid.

By using constitutive equation, Eq. (14), and Green's theorem weak form equation can be written as below:

$$\int_{V_f}\left[\delta p\left(\frac{1}{K_f}\ddot{p}+\frac{\gamma}{\rho_f K_f}\dot{p}\right)+\frac{1}{\rho_f}\frac{\partial}{\partial \mathbf{x}}\delta p\cdot\frac{\partial}{\partial \mathbf{x}}p\right]dV - \int_S \delta p(T(\mathbf{x}))ds = 0 \tag{15}$$

where

$$T(\mathbf{x}) = -\mathbf{n}\cdot\left(\frac{1}{\rho_f}\frac{\partial}{\partial \mathbf{x}}p\right). \tag{16}$$

And the vector $\mathbf{n}$ represents the inward normal to the acoustic medium at the boundary.

The last term in Eq. (15) introduces the boundary condition statement for the acoustic problems. All of the boundary conditions described below can be formulated in terms of T(x) – this term has dimensions of acceleration.

There are two boundary conditions in this paper: the infinite boundary condition and the boundary condition on the interface of spheres and air. Only these boundary conditions are studied here. The problem is simulated as an outdoor problem so that the boundary condition, in outer surface of finite elements, has to act as an infinite medium. This boundary condition usually is obtained from using infinite elements or from a proper choice of impedance coefficients. Only the second method is taken into consideration in this research.

To use impedance condition we have to define impedance condition so that there is not any reflection from the surface so that it can be written as below [16]:

$$T(\mathbf{x}) = -\left(\frac{1}{c_1}\dot{p} + \frac{1}{a_1}p\right) \tag{17}$$

where

$$\frac{1}{c_1} = \frac{1}{\sqrt{\rho_f K_f}}$$
$$\frac{1}{a_1} = \frac{1}{2\rho_f r_1} + \frac{\gamma}{2\rho_f\sqrt{\rho_f K_f}}. \tag{18}$$

In these equations r_1 refers to the radius of curvature of the boundary.

Another boundary condition that exists in the simulation is the boundary of air with spheres. In these boundaries, based on continuity law, it is assumed that acoustic and structure media have the same displacement normal to the boundary. So that for this boundary Eq. (19) can be written.

$$T(\mathbf{x}) = \mathbf{n}\cdot\left(\ddot{\mathbf{u}}^m + \frac{\gamma}{\rho_f}\dot{\mathbf{u}}^m\right). \tag{19}$$

In the great majority of practical applications the acoustic tractions associated with volumetric drag are small compared to those associated with the fluid inertia, so that this term is ignored in transient analysis. In this condition the effects of surface velocity can be ignored. Therefore we can assume that only acceleration of surface excites the air. The Rayleigh's surface integral uses this assumption as well [19]. By neglecting volumetric drag and omitting extra terms, Eq. (15) can be discretized as follows:

$$M_f^{PQ}\ddot{p}^Q + C_{fr}^{PQ}\dot{p}^Q + \left(K_f^{PQ} + K_{fi}^{PQ}\right)p^Q - S_{fs}^{PM}\ddot{u}^M = 0. \tag{20}$$

If $p = H^P p^P$ is used to interpolate the pressure and $\mathbf{u}^m = N^N u^N$ is used to interpolate the displacement then the terms of Eq. (20) can be calculated by following relations [16]:

$$M_f^{PQ} = \int_{V_f}\frac{1}{K_f}H^P H^P dV \tag{21}$$

$$C_{fr}^{PQ} = \int_{S_{fr}\cup S_{frs}}\left(\frac{\gamma}{\rho_f}\frac{1}{k_1} + \frac{1}{c_1}\right)H^P H^P dS + \int_{S_{fi}}\frac{1}{c_1}H^P H^P dS \tag{22}$$

$$K_f^{PQ} = \int_{V_f}\frac{1}{\rho_f}\frac{\partial H^P}{\partial \mathbf{x}}\cdot\frac{\partial H^Q}{\partial \mathbf{x}}dV \tag{23}$$

$$K_{fi}^{PQ} = \int_{S_{fi}}\frac{1}{a_1}H^P H^P dS \tag{24}$$

$$S_{fs}^{PM} = \int_{S_{fr}\cup S_{frs}}H^P\mathbf{n}\cdot N^M dS. \tag{25}$$

Acceleration was calculated in previous section. By substitution calculated acceleration into Eq. (20), the pressure field will be remained unknown. ABAQUS software has been used

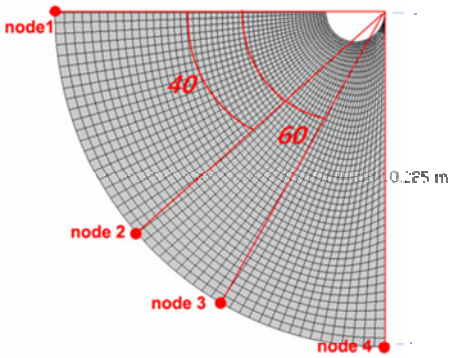

Fig. 6. Acoustic mesh.

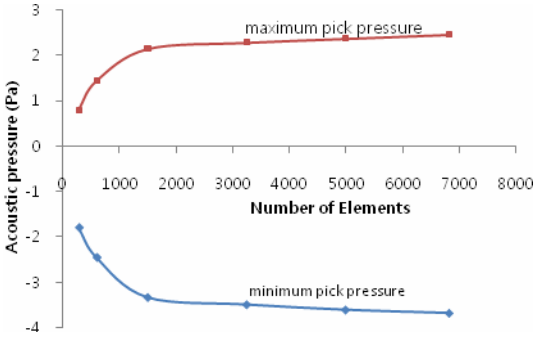

Fig. 7. Acoustic mesh convergence.

to solve Eq. (20) and predict the acoustic pressure. The model is discretized utilizing 3500 acoustic element with one Gaussian integration point as shown in Fig. 6. The biggest element in this mesh has 9 millimeters length. For the first order elements (linear shape functions), the element dimensions have to be chosen such that the biggest one is at least six times smaller than the acoustic wavelength [20]. As it is shown in Fig. 4(b), all of audible waves have frequency less than 6 kHz. Based on these frequencies, presented mesh has suitable size. Fig. 7 shows the minimum and the maximum of sound pressure that was sensed in node 1 for different meshes. This Figure also confirms the mesh. After solving the Eq. (20), by explicit method, we can gain the sound pressure contour as shown in Fig. 8.

Fig. 9 shows the pressure time history for different nodes that are depicted in Fig. 6. In this figure the solid line illustrates FEM results, dot line shows theoretical results, and dash line was created by experiment. This figure shows a fairly good agreement between acoustical simulation results and experimental data. As for this figure, the finite element error to express pressure is less than 1.5 dB. FEM gives a wave very similar to experiment in all of the nodes but accuracy of theoretical result decreases by getting away from impact axis. Theoretical errors are created by the reflection of sound between the spheres. In the superposition that is applied in theoretical method, the reflection of the sound is ignored. The little error of the simulation possibly is occurred by inaccurate material properties that are used in the simulation.

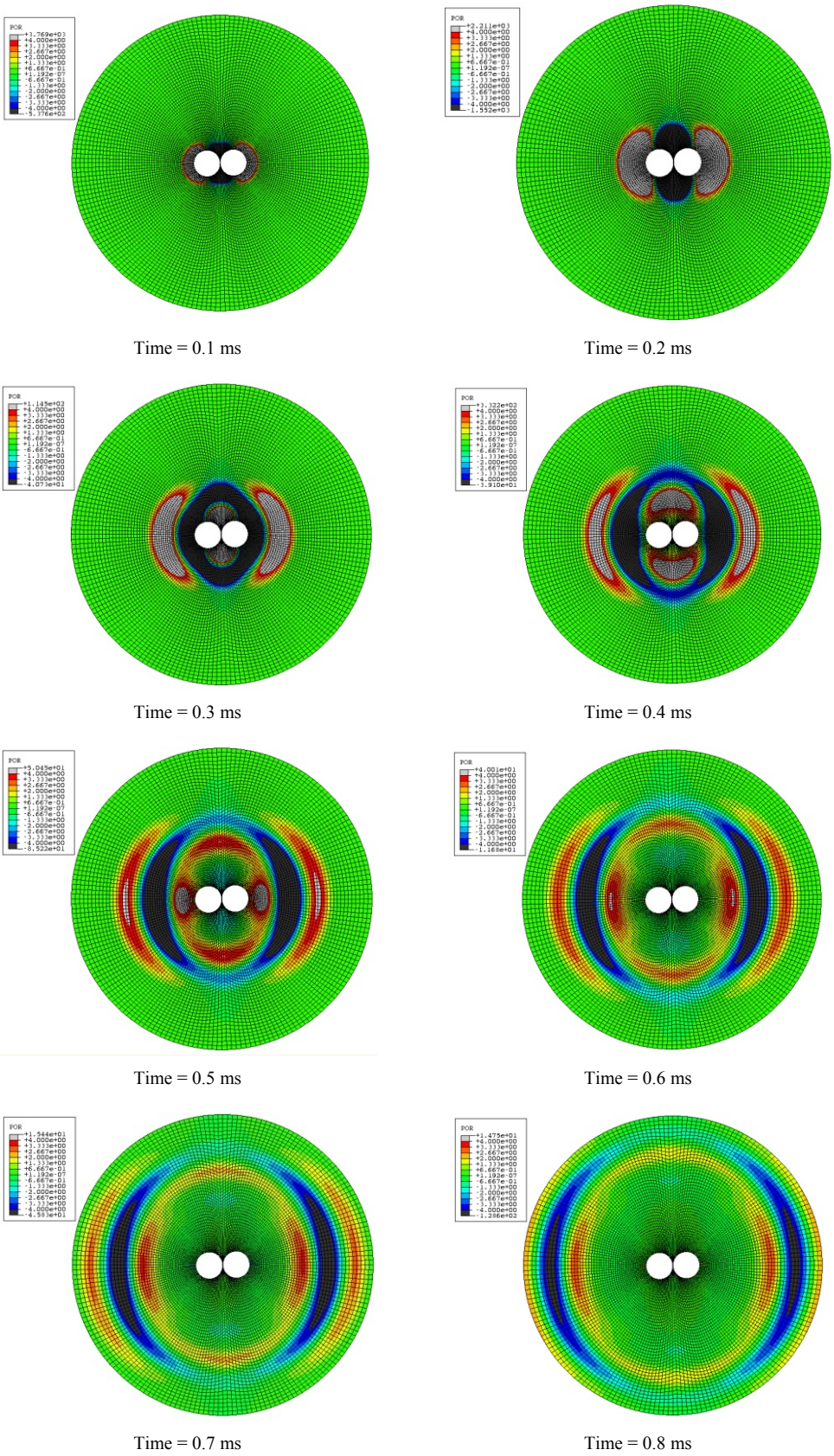

Time = 0.1 ms | Time = 0.2 ms

Time = 0.3 ms | Time = 0.4 ms

Time = 0.5 ms | Time = 0.6 ms

Time = 0.7 ms | Time = 0.8 ms

Fig. 8. Acoustic pressure field propagation.

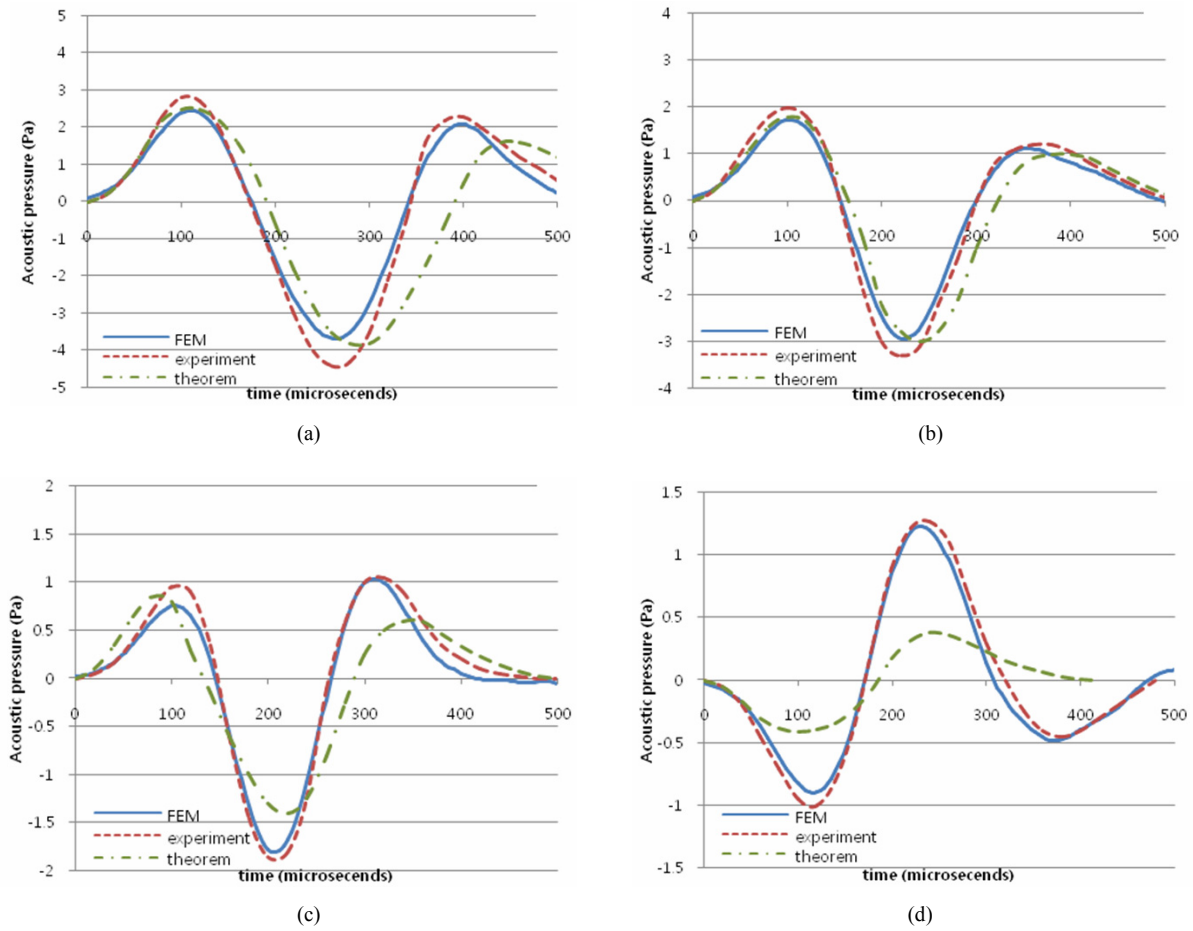

Fig. 9. Sound pressure (a) node 1; (b) node 2; (c) node 3; (d) node 4.

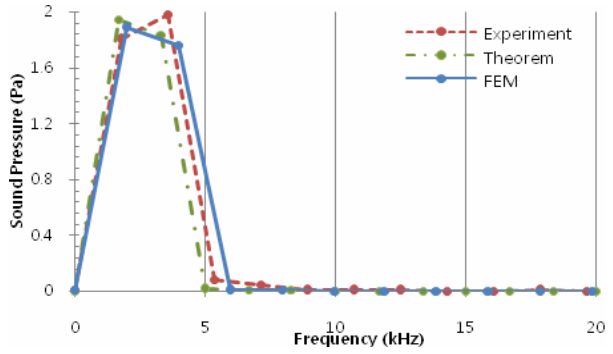

Fig. 10. Sound spectrum in node 1.

Koss and Alfredson [12] observed that if the sound spectrum is studied then the intense signal has a frequency that is given by:

$$f = \frac{76.1}{a}\ Hz = 2996\ Hz \tag{26}$$

where a is the radius of spheres. To study this relation we have to plot sound spectrum. The results of Fourier transform is shown in Fig. 10.

This figure validates the Eq. (26). If sound spectrum is plotted for other points of the model then it can be shown that the most intense signal has similar frequency.

In the beginning of section 3, the effects of air on sphere are neglected, because of difference of elastic wave speed in the air (340 m/s) and in the steel (5060 m/s). We should study the energy of radiated sound to demonstrate this subject. This energy is radiated from spheres but it was ignored in the first step of simulation. Fig. 11 shows the sound power that is passing through boundary of acoustic elements.

To evaluate all of radiated energy, this curve should be integrated. The integration shows that 0.7 micro joule of energy was radiated as sound due to the impact. To justify neglecting of this amount of energy, we should say that initial kinematic energy is 24 millijoules. This means that only $\frac{1}{35000}$ of initial energy of system is lost. Therefore we can assume that energy is not transferred to air. In addition to that, we can ignore the air effects.

4. Modal analysis

The vibration modes of the spheres was explained in the previous sections. In this section natural frequency of the

Table 1. Natural frequencies of the sphere.

Mode number	Natural frequency (kHz)
1	51.8
2	68.3
3	77.0
4	93.1
5	97.0
6	98.5
7	118.7
8	128.2
9	136.7
10	138.3

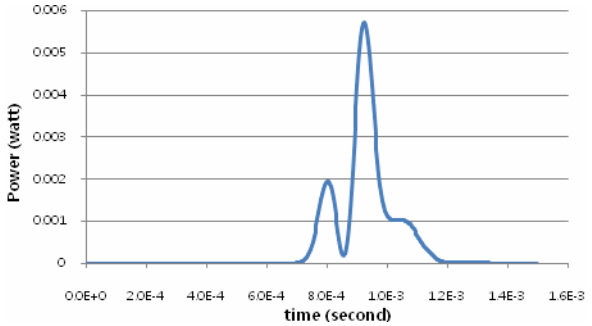

Fig. 11. Sound power radiated from spheres.

spheres will be calculated. Eq. (27) is used to determine the natural frequencies and mode shapes.

$$(-\omega^2\mathbf{M}+\mathbf{K})\boldsymbol{\varphi}=0 \tag{27}$$

where ω shows an eigenvalue (or natural frequency), $\boldsymbol{\varphi}$ is an eigenvector, **M**, and **K** are mass matrix and stiffness elastic matrix of the sphere, respectively. These matrices are calculated for an element as follows:

$$M^{NM}=\int_V \rho N^N.N^M dV \tag{28}$$

$$K^{MN}=2\pi\int \mathbf{B}^T\mathbf{D}\mathbf{B}\,r\,dr\,dz. \tag{29}$$

With using Eq. (27), first 10 natural frequencies of the sphere are obtained and show in Table 1.

Although basics of calculation that was used here is different with dynamical analysis in section 3.1, it is clear that these frequencies is merged on picks of Fig. 4(b) this coincidence shows the influence of Fourier transform and the modal analysis.

5. Effects of vibration modes on radiation of sound

It was mentioned that the base frequency of the sphere is 51 kHz. So the vibrational modes cannot play any role in radiation of audible sound.

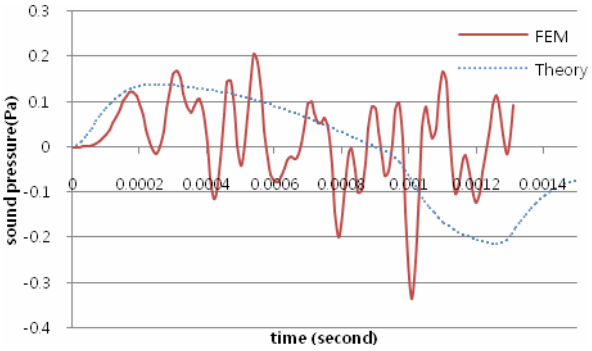

Fig. 12. Radiated acoustic pressure from softened spheres.

Koss and Alfredson ignored vibration to drive their relations. In other words, they can just study the noise of rigid body motion. Survey of vibration role in sound creation is not possible theoretically; especially if this transient vibration was created by a complex force such as impact.

Here a new problem is studied with finite element method. The problem is similar to previous problem, but to decrease natural frequencies, the prior Young's module is divided by 100. Natural frequencies are reduced 10 times by decreasing of Young's module. So in this new condition if the impact excites the vibrational modes then the modes can affect on radiated noise. In this section, vibration modes affect the results so acoustic medium is meshed by acoustic element with finer size.

Fig. 12 shows the acoustic pressure in a state on impact axis and 0.285 meter far from impact point. In the figure the solid line is based on FEM and dot-line is based on Koss and Alfredson relations.

The Fig. 12 also illustrates that the pick of theoretical pressure is -0.21 Pa. On the other hand, FEM expresses pick pressure equal to -0.34 Pa. In this figure it is clear that theoretical relations cannot predict shape of the wave correctly. Although all of these waves are created during contact time, which is 1.25 ms, we cannot see one half-sine signal in this figure. It is maybe seen that the sound is very weak in this condition. It means that the noise does not make any differences when materials have this amount of Young's module. We should say that decrease of Young's module is just a symbolic change to study effect of vibrational modes if vibrations have a role in creation of sound. Richards et al. [14] express that if effective radius ($\sqrt{(\text{surface area})/4\pi}$) is used instead of radius, the theorem can be used for more complex bodies. So in the practical works, such as plates, beams and tubes, it is possible that vibrational modes be in the range of audible sound and play a role in sound generation. This has been investigated by Fallstrom et al. and Olofsson et al. [21, 22].

We can study the sound spectrum to find more about effects of modes. Fig. 13 shows the Fourier transform of acoustic pressure curves shown in Fig. 12.

As expected if the vibrations have an effect in the created

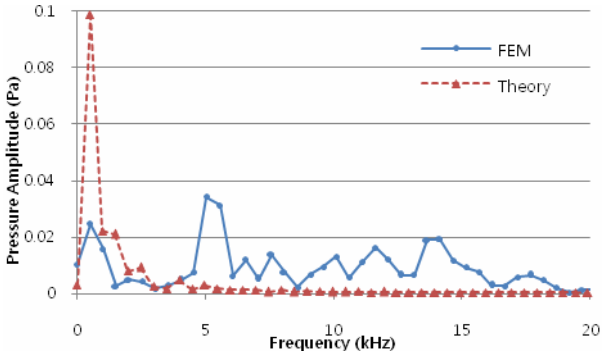

Fig. 13. Sound spectrum for softened spheres.

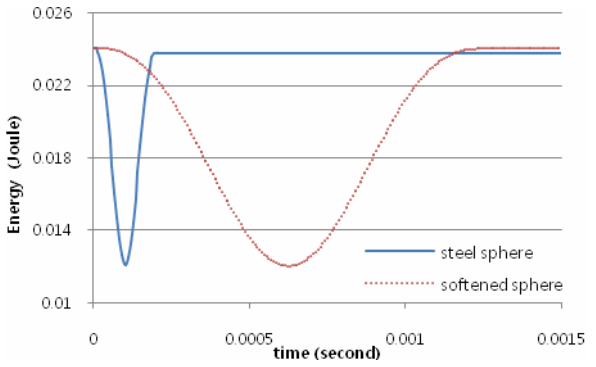

Fig. 14. Kinetic energy in the colliding spheres.

sound, the theoretical method will be insecure. Fig. 13 shows that the vibrational modes raise the intensity of waves that their frequencies are more than 4 kHz and this is due to the fact that the natural frequencies of spheres have this range of frequency as well. So it is important to study the vibrational modes before using any theoretical relations.

Koss and Alfredson derived that since the amount of energy is partitioned into natural mode of the spheres is small in comparison to original kinetic energy of sphere, the effects of modal vibrations within the sphere in sound radiation can be neglected. Fig. 14 shows the kinetic energy for surveyed spheres. In this figure solid line shows kinetic energy for steel sphere and dot-line shows kinetic energy for softened sphere.

We know that after impact happens, some of the kinetic energy is stored in the spheres as elastic energy. This amount of energy is partitioned to the vibration modes. Fig. 14 shows that this energy is neglected in comparison to original kinetic energy. We can also see that 0.15 percent of original kinetic energy leaves in softened sphere and 1.1 percent of original kinetic energy leaves in steel sphere. Although partitioned energy in softened sphere is very small, Fig. 13 shows that vibrations have more significant role in radiation of audible sound in comparison to the rigid body motion. It is seen that the partitioned kinetic energy is not suitable criterion to judge about contribution of vibration modes in the sound field. That is because of the fact that radiated sound is created by the surface acceleration but not due to the kinetic energy. We can also see that although partitioned energy in steel sphere is more than the softened sphere, the radiated sound from the steel sphere due to the vibrations is not in the audible range.

6. Conclusions

Results show the ability of finite element to model impact noise. Nonetheless, because of complexities of interactions, the meshing needs so attention to arrive admissible results. In some manuscripts, it is said that for the first order acoustic elements, the elements size must be six times smaller than the acoustic wave length. Studding mesh sensitivity analysis for this problem shows that if coincidence between solid elements and acoustic elements does not make an error, this limitation governs as well.

Although Fig. 4(b) shows that there are some acceleration waves with frequency more than 50 kHz, we cannot see pressure waves in this range of frequency. It is because of unsuitable elements size to model this range of frequency. Since measuring equipments cannot record waves with frequency above 20 kHz, we cannot see high frequency waves in the experimental data either.

When the steel spheres collide, 1.1 percent of the impact energy is stored in the spheres as vibrational energy. Also, when the softened spheres collide, 0.15 percent of the impact energy was transformed to the vibration. Results also show that the vibrations of steel spheres do not have any role in creation of audible sound. While, not only vibrations of softened spheres create sound but also the vibration modes have more significant effect in the sound generation than rigid body motion. Therefore, we cannot judge about the contribution of vibration modes in creation of sound by use of the partitioned kinetic energy in the modes.

Results show the limitation of the Hertz theory to predict acoustic radiation. It also depicts that since impact excites all of vibration modes, we cannot neglect effects of vibration in sound field if vibration modes have frequency in audible range. When a body with a complex shape is impacted, if vibration modes are not in audible range, we can just assume that sound is radiated due to the rigid body acceleration. Only in this condition we can use viewpoint of Richards et al to estimate sound field by replacing effective radius into Koss and Alfredson theorem.

Nomenclature

a : Radius of sphere
c : Speed of sound in air
E : Elasticity modulus
E_* : Effective elasticity modulus
H^p : Pressure interpolator function
$\mathbf{I}^N$: Internal force vector
K_f : Bulk modulus of fluid

m : Mass of sphere
m_* : Effective mass
$\mathbf{M}^{NM}$: Mass matrix
$\mathbf{n}$: Normal to surface
$\mathbf{N}^N$: Displacement interpolator function
p : Pressure
$\mathbf{p}^N$: External force vector
r : Distance from impact point
r_1 : Radius of boundary curvature
R_* : Effective radius
t : Time
$\mathbf{t}$: Surface traction
t' : Delay time
$\mathbf{u}^f$: Fluid displacement
$\dot{\mathbf{u}}^f$: Fluid velocity
$\ddot{\mathbf{u}}^f$: Fluid acceleration
$\dot{\mathbf{u}}^m$: Velocity of material
$\ddot{\mathbf{u}}^m$: Acceleration of material
v_0 : Impact velocity
$\mathbf{x}$: Point coordinate
α_c : Mass of Rayleigh damping
$\boldsymbol{\beta}^N$: Strain interpolator function
γ : Volumetric drag
δp : Pressure variation
$\delta\mathbf{u}^m$: Variation displacement field
$\delta\boldsymbol{\varepsilon}$: Strain variation field
θ : Degree from impact axes
ρ : Density
ρ_0 : Air density
ρ_f : Density of fluid
$\boldsymbol{\sigma}$: Stress tensor
τ : Impact duration
v : Poisson's ratio
$\boldsymbol{\varphi}$: Natural modes
ω : Natural frequency

References

[1] K. E. Fallstrom, H. Gustavsson, N. E. Molin and A. O. Wahlin, Transient bending waves in plates studied by hologram interferometry, *Experimental Mechanics*, 29 (4) (1989) 378-387.

[2] K. E. Fallstrom, L. E. Lindgren, N. E. Molin and A. O. Wahlin, Transient bending waves in anisotropic plates studied by hologram interferometry, *Experimental Mechanics*, 29 (4) (1989) 409-413.

[3] S. L. Lopatnikov, B. A. Gama, M. J. Haque, C. Krauthauser and J. W. Gillespie Jr, High-velocity plate impact of metal foams, *International Journal of impact engineering*, 30 (2004) 421-445.

[4] A. O. Wahlin, P. O. Gren and N. E. Molin, On structure-borne sound: Experiments showing the initial transient acoustic wave field generated by an impacted plate, *Journal of the Acoustic Society of Americ*a, 96 (5) (1994) 2791-2797.

[5] S. Schedin, C. Lambourge and A. Chaigne, Transient sound fields from impacted plates: comparison between numerical simulations and experiments, *Journal of Sound and Vibration,* 221(3) (1999) 471-490.

[6] A. Ross and G. Ostiguy, Propagation of the initial transient noise from an impacted plate, *Journal of Sound and Vibration,* 301 (2007) 28-42.

[7] K. Olofsson and L. E. Lindgren, Holographic interferometry measurements of transient bending waves in tubes and rings, *Experimental Mechanics,* 33 (4) (1993) 308-313.

[8] K. Olofsson, K. E. Fällström and P. Palágyi, Laser generated and recorded transient bending waves in composite tubes, *Journal of Experimental Mechanics,* 36 (3) (1996) 224-231.

[9] A. Love, *A treatise on the mathematical theory of elasticity*, Fourth edition, New York, Dover Publications (1944) 198.

[10] W. Goldsmith, *Impact*, London, Edward Arnold (1960) Chapter 4.

[11] G. Nishimura and K. Takahashi, Impact sound by mutual collision of two steel balls, *Bulletin of the Japan Society of Precision Engineers,* 1 (1965) 47-51.

[12] L. L. Koss and R. J. Alfredson, Transient sound radiated by spheres undergoing an elastic collision, *Journal of Sound and Vibration*, 27 (l) (1973) 59-75.

[13] W. Yufang and T. Zhongfang, Sound radiated from the impact of two cylinders, *Journal of Sound and Vibration,* 159 (2) (1992) 295-303.

[14] E. J. Richards, M. E. Westcott and R. K. Jeyapalan, On the prediction of impact noise I: Acceleration noise, *Journal of Sound and Vibration,* 62 (4) (1979) 547-575.

[15] L. Rayleigh, On the production of vibrations by forces of relatively long duration with the application to the theory of collisions, *Edinburgh and Dublin Philosophical Magazine*, Sixth Series (2) (1906).

[16] ABAQUS Theory Manual, v6.6 (2006).

[17] H. Deresiewicz, A note on Hertz's theory of impact, *Acta Mechanica,* 6 (1) (1968) 110-112.

[18] R. F. Barron, *Industrial noise control and acoustics*, USA, Marcel Dekker (2003) ISBN 0-824-70701-X.

[19] A. Akay and M. Latcha, Sound radiation from an impact-excited clamped circular plate in an infinite baffle, *Journal of the Acoustical Society of America,* 74 (2) (1983) 640-648.

[20] T. Łodygowski and W. Sumelka, Limitations in application of finite element method in acoustic numerical simulation, *Journal of Theoretical and Applied Mechanics,* 44 (4) (2006) 849-865.

[21] K. E. Fallstrom, L. E. Lindgren, N. E. Molin and A. O. Wahlin, Transient bending waves in anisotropic plates studied by hologram interferometry, *Exp. Mech.,* 29 (4) (1989) 409-413.

[22] K. Olofsson and L. E. Lindgren, Holographic interferometery measurements of transient bending waves in tubes and rings, *Exp. Mech.,* 33 (4) (1993) 308-313.

Kamran Mehraby holds a bachelor degree in Mechanical Engineering from Azad University of Khomeinishahr, Khomeinishahr, Isfahan, Iran, and M.Sc. in Mechanical Engineering from Shahrekord University, Shahrekord, Iran in 2010. His research interests include: metal forming, structural dynamics, mechanical impacts, shock-absorbers, mechanical vibration, and vibro-acoustic. He deliberated to control noise of shock-absorbers from 2007 to 2010.

Hamid Kh. Beheshti is an assistant professor of the Mechanical Engineering at the University of Isfahan, Isfahan, Iran. His research interests include structural dynamics, aeroelasticity, automotive and aircraft crashworthiness, occupant protection, and injury biomechanics. He received the B.Sc. and M.Sc. degrees in mechanical engineering from Isfahan University of Technology, Isfahan, Iran in 1994 and 1998, respectively. He received the Ph.D from Wichita State University, Wichita, Kansas, USA in 2004. He was a research assistant in National Institute for Aviation Research from 2000 to 2004. He worked as a dynamics and loads engineer in dynamics loads group at Cessna Aircraft Company, mostly involved with landing gear design and aircraft dynamic load calculation from 2004 to 2006.